tion of the viscometer body, cm.

l' = $4V/\pi D_1^2$ = volume equivalent length of the viscometer body, cm.

N_{Re} = $D_e v\rho/\mu$ = Reynolds number, dimensionless

p = pressure, lb./sq. in. gauge

t = temperature, °C.

V = volume of the viscometer body, cc.

v = terminal velocity of the falling body, cm./sec.

Greek Letters

α = temperature coefficient of the viscometer constant, $(°C.)^{-1}$

β = viscometer constant defined by Equation (1), cc./sec.^{2}

β_{isf} = viscometer constant defined by Equation (2), cc./sec.^{2}

$\beta_{(t,p)}$ = viscometer constant of Equation (1) as a function of temperature and pressure, cc./sec.^{2}

$\beta_{(0,0)}$ = viscometer constant of Equation (1) corrected to 0°C. and 1 atm., cc./sec.^{2}

γ = pressure coefficient of the viscometer constant, (lb./sq.in. gauge)$^{-1}$

μ = absolute viscosity, poise or g.-mass/cm.-sec.

ρ = fluid density, g.-mass/cc.

σ = density of the viscometer body, g.-mass/cc.

ϕ = general function

LITERATURE CITED

1. Bridgman, P. W., *Proc. Am. Acad. Arts Sci.*, **61**, 57 (1926).
2. *Ibid.*, **66**, 185 (1931).
3. Hilsenrath, J., et al., *Circular 564*, National Bureau of Standards, Washington, D. C. (1955).
4. Kestin, J., "Transport Properties of Gases," p. 27, Northwestern University Press, Evanston, Illinois (1958).
5. ———, and H. E. Wang, *Physica*, **24**, 694 (1958).
6. Lohrenz, John, Ph.D. thesis, University of Kansas, Lawrence, Kansas (September, 1960).
7. ———, G. W. Swift, and Fred Kurata, *A.I.Ch.E. Journal*, **6**, 547 (1960).
8. Michels, A., and R. O. Gibson, *Proc. Roy. Soc. (London)*, **134A**, 288 (1932).
9. Ross, J. F., and G. M Brown, *Ind. Eng. Chem.*, **49**, 2026 (1957).
10. Rossini, F. D., director, "Selected Values of the Properties of Hydrocarbons and Related Compounds," Carnegie Institute of Technology, Pittsburgh, Pennsylvania (1959).
11. Sage, B. H, and W. N. Lacey, *Ind. Eng. Chem.*, **30**, 829 (1938).
12. Swift, G. W., Ph.D. thesis, University of Kansas, Lawrence, Kansas (June, 1959).
13. ———, John Lohrenz, and Fred Kurata, *A.I.Ch.E. Journal*, **6**, 415 (1960).

Manuscript received March 16, 1961; revision received September 15, 1961; paper accepted September 19, 1961.

The Photochlorination of Chloroform in Continuous Flow Systems

JAMES E. HUFF and CHARLES A. WALKER

Yale University, New Haven, Connecticut

Data on the vapor phase photochlorination of chloroform in flow reactors are interpreted on the basis of reaction mechanisms presented in the literature. In order to estimate the rates of light absorption it is also necessary to interpret the rate data obtained for the uranyl sulfate-oxalic acid reaction.

The chlorination results are represented quite well by a mechanism in which the most important termination step is a termolecular reaction between trichloromethyl radicals and chlorine. Deviations from this model are observed as the flow of reactants becomes turbulent and as the light intensity increases. The observed decrease in reaction rate under such conditions is attributed to the increased significance of a second termination step, the unimolecular deactivation of chlorine radicals at the reactor wall.

Photochemical reactions have been carried out on a commercial scale for many years. It is somewhat surprising then that publications concerning the problem of photoreactor design have begun to appear only recently. The most comprehensive of these recent papers is that of Doede and Walker (*4*). These authors review the fundamentals of photochemical kinetics and show qualitatively how these principles apply to the design of practical photoreactors. No quantitative design relationships are presented in this general paper.

Governale and Clarke (*7*) have presented an interesting history of the development of a commercial photoreactor. The information presented in this paper is largely qualitative, and little is said concerning the application of photochemical and kinetic fundamentals to the problem of scale-up and design.

A more fundamental study of the problem of reactor design was carried out by Baginski (*2*), who studied the addition of hydrogen sulfide to terminal olefins in continuous photoreactors. Unfortunately severe back mixing due to density gradients precluded a detailed interpretation of the results. More recently Gaertner and Kent (*5*) have studied the oxalic acid-uranyl nitrate photolysis in a continuous reactor. These authors rely heavily on physical and kinetic principles in their analysis of the results. However their differential rate equation, though based on classical photochemical laws, is somewhat inconsistent with modern kinetic theory.

An analytical representation of the kinetics of a photoreaction taking place in an isothermal, laminar-flow reactor has been developed by Schechter and Wissler (*11*). Their equations apply only for a reaction first order in light intensity and reactant concentration, and in which the absorbing species is not consumed (photosensitized system). The effect of diffusion and light attenuation on observed over-all conversions are considered in this analysis. No experimental work is presented.

The present study arose from questions regarding the proper methods of application of the theory to the design of photoreactors. It is the purpose of this paper to present data on the vapor-phase photochlorination of chlo-

James E. Huff is with Dow Chemical Co., Midland, Michigan.

roform in a flow system and to apply theoretical principles in the interpretation of the results. The interpretive models used in this analysis might well find application in problems of design and scale-up.

KINETICS OF THE PHOTOCHLORINATION OF CHLOROFORM

The chlorine-chloroform reaction was chosen for study primarily because of the knowledge that has accumulated on the mechanism of the reaction. Previous investigators have reported that the following reactions likely occur under 3,000 to 5,000Å. light:

Initiation:

$$Cl_2 \xrightarrow{k_1 I_a} 2\,Cl\cdot \qquad (1)$$

Propagation

$$Cl\cdot + CHCl_3 \xrightarrow{k_2} CCl_3\cdot + HCl \qquad (2)$$

$$CCl_3\cdot + HCl \xrightarrow{k_3} Cl\cdot + CHCl_3 \qquad (3)$$

$$CCl_3\cdot + Cl_2 \xrightarrow{k_4} CCl_4 + Cl\cdot \qquad (4)$$

Termination

$$2\,CCl_3\cdot + Cl_2 \xrightarrow{k_5} 2\,CCl_4 \qquad (5)$$

$$Cl\cdot + \text{wall} \xrightarrow{k_6} \tfrac{1}{2}\,Cl_2 \qquad (6)$$

$$2\,CCl_3\cdot \xrightarrow{k_7} C_2Cl_6 \qquad (7)$$

There is little doubt that reaction 1 is the proper initiation step, or that reaction 2 is the process by which trichloromethyl radicals and hydrogen chloride are formed. However there is some disagreement in the literature as to whether the rate of reaction 3 (reverse of 2) is significant with respect to the rate of the forward reaction. In their studies of the vapor-phase reaction Schumaker and Wolf (*12*) and Winning (*14*) found it unnecessary to consider step 3 in the interpretation of their results. The same conclusion was reached by Beezhold and Ornstein (*3*) in their study of the reaction in the liquid phase. However Schwab and Heyde (*13*) (liquid phase) and Newton and Rollefson (*8*) (vapor phase) found it necessary to consider step 3 in order to adequately explain their results. The latter investigators carried out an ingenious isotope-exchange experiment to demonstrate that the occurrence of this reaction can be detected. The position of the equilibrium was not determined however.

Reaction 4 is generally accepted as the step by which chlorine radicals are regenerated, and step 5 and/or 6 have been shown to be the predominant termination reactions. The possibility that reaction 7 may be an important step was pointed out in one paper

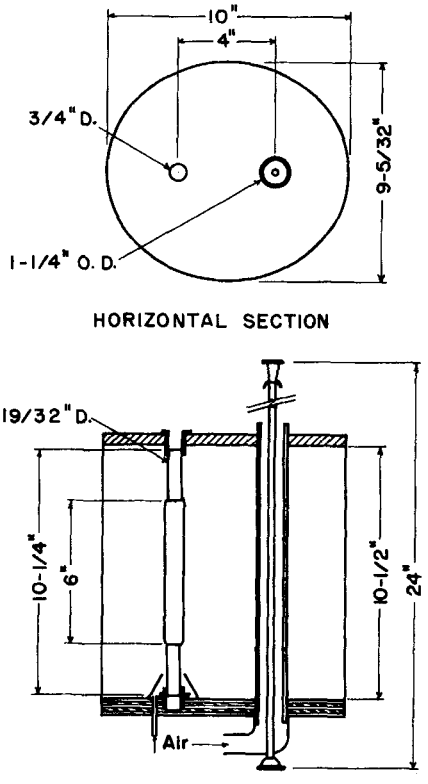

Fig. 1. Reactor system.

(*8*), but no other investigators have given evidence to support this contention. Winning (*14*) rules out this step as being an important mechanism of termination.

In the light of this past work it can be concluded that a general derivation of the over-all rate equation should include the first six reactions of the mechanism, but probably not the last step. On this basis expressions may be written for the net rate of formation of chlorine radicals $[d(Cl\cdot)/dt]$ and of trichloromethyl radicals $[d(CCl_3\cdot)/dt]$ and for the over-all reaction rate $[d(HCl)/dt]$. For the stationary state period (when rates of change of free radical concentrations are considered negligible) the following expression is obtained:

$$d(HCl)/dt = \frac{2k_1 k_2 (CHCl_3) I_a}{k_2(CHCl_3) + k_6} + \left\{ \frac{k_2 k_4 (Cl_2)(CHCl_3) - k_3 k_3 (HCl)}{4k_5 (Cl_2)[k_2(CHCl_3) + k_6]} \right\}$$

$$\left\{ \sqrt{\left[k_6 \frac{k_3(HCl) + k_4(Cl_2)}{k_2(CHCl_3) + k_6} \right]^2 + \frac{16 k_1 k_2 k_5 (Cl_2)(CHCl_3) I_a}{k_2(CHCl_3) + k_6}} - k_6 \frac{k_3(HCl) + k_4(Cl_2)}{k_2(CHCl_3) + k_6} \right\} \qquad (8)$$

The mechanisms that are predominant in the literature (*3, 12, 14*) are based on the assumption that the homogeneous termination (reaction 5) is the predominant deactivation step.

In two papers (*3, 12*), steps 3 and 6 are both omitted in the derivation. It is interesting to observe that if k_6 is set equal to zero, Equation (8) reduces to

$$d(HCl)/dt = 2k_1 I_a + k_4 \sqrt{\frac{k_1}{k_5}(Cl_2) I_a} \qquad (9)$$

Equation (9) is identical to the literature equations. Based on this mechanism, the rate of step 3 can have no influence on the over-all rate, when experimental conditions are such that the rate of step 6 is small with respect to that of step 5.

Under certain experimental conditions reaction 6 must be considered as the predominant termination step (*13*). By proper algebraic manipulation of Equation (8) k_5 can be taken to the limit of zero, and

$$d(HCl)/dt = \frac{2k_1 k_2 k_4 (Cl_2)(CHCl_3) I_a}{k_6[k_3(HCl) + k_4(Cl_2)]} \qquad (10)$$

Equation (10) is in agreement with that presented in the literature. In the original paper the rate of initiation is represented by $k_1' I_a (Cl_2)$, rather than by $2k_1 I_a$ (permissible for weak absorption).

One of the purposes of the present work is to determine whether either of the mechanisms represented by Equations (9) and (10) can be used to interpret experimental data obtained from a flow system. This requires consideration of the significance of the term I_a in a flow system. Considering reaction 1 one will note that the dimensions of I_a will be Einsteins/sec. cc. if concentrations are in moles/cc., time is sec. and quantum efficiency is moles reacted/Einstein adsorbed. Thus I_a is the rate of light absorption per unit volume of reacting mixture.

Consider a reactor of cylindrical cross section evenly illuminated from the outside. Assume that all light rays pass perpendicularly through the axis of the tube and that concentrations and velocity are essentially constant over the cross section. In the thin-walled cylinder between r and $r + dr$ the fractional absorption of light as given by the Beer-Lambert law is

$$\frac{dn_a}{n_o} = kC\left[e^{-kC(R-r)} + e^{-kC(R+r)}\right] dr \qquad (11)$$

The fractional absorption of light over the reactor is given by integrating this expression from 0 to R:

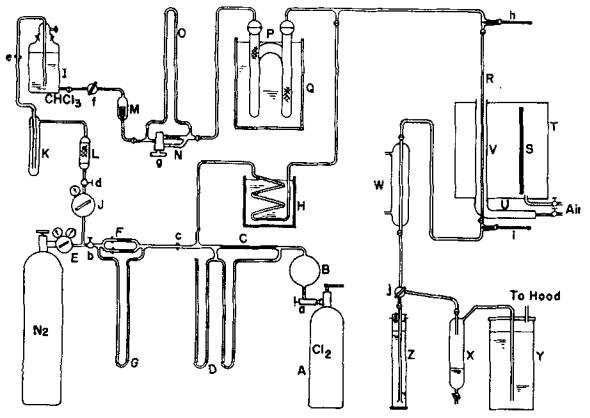

Fig. 2. Experimental equipment.

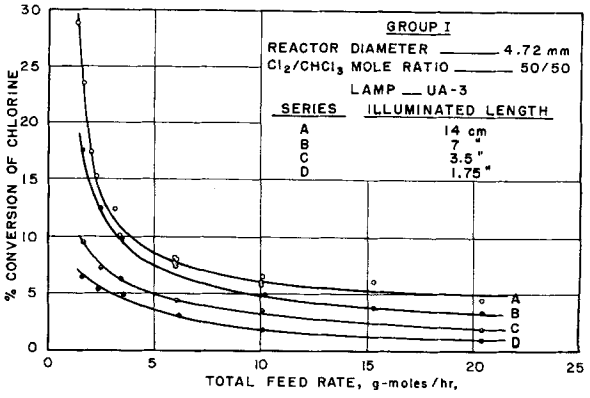

Fig. 3. Variation of reactor length, group I.

$$\frac{n_a}{n_o} = 1 - e^{-k\,C\,D} \qquad (12)$$

In this work the term I_a is calculated as an average rate of light absorption per unit volume by a procedure which includes (a) determination of n_o, the light incident on the inside wall of a reactor, by use of the uranyl sulfate-oxalic acid actinometer, (b) calculation of the rate of light absorption by Equation (12), and (c) dividing the rate of light absorption by the reactor volume, $\pi R^2 L$.

The term I_a is given more rigorously by dividing Equation (11) by the volume of a ring of differential thickness to obtain

$$\frac{d\,n_a}{d\,V} = I_a = \frac{n_o\,k\,C\,[e^{-k\,C(R-r)} + e^{-k\,C(R+r)}]}{2\pi\,r\,L} \qquad (13)$$

Thus the rate of absorption of light per unit volume is a function of radial distance r. Hence the reaction rate in each thin-walled element should be calculated by using Equation (13) in a rate equation and the over-all result obtained by the appropriate integration procedure.

The error involved by using the average rate of light absorption per unit volume was estimated for cases of low fractional absorption of light (as in the chlorination runs of this work) by using the first two terms of the McLaurin series expansion of the Beer-Lambert law:

$$n_t/n_o \equiv 1 - k\,C\,d \qquad (14)$$

When one uses this equation, the fractional absorption of light in a ring of thickness dr is simply

$$dn_a/n_o = 2\,k\,C\,dr \qquad (15)$$

This equation was used to calculate I_a on two bases: (a) I_a was calculated as the rate of light absorption per unit volume in a differential ring, and (b) I_a was calculated as an average value by integrating Equation (15) and then dividing by $\pi R^2 L$. When these values of I_a were used appropriately in Equation (9) with the term $2\,k_1\,I_a$ omitted (see later discussion), it was found that the average concentration gradients predicted by the two approaches differed by less than 10%.

EXPERIMENTAL EQUIPMENT AND PROCEDURES

The experimental apparatus is shown in Figure 1. Cylinder chlorine flows through a needle valve (a) and a surge bottle (A) and is metered by means of capillary tubes (B) and carbon tetrachloride manometers (C). Prepurified cylinder nitrogen can be metered into the chlorine stream by means of a second capillary meter system (D). The mixed chlorine-nitrogen stream, preheated in a 120°C. oil bath (E), then flows through heated glass lines to a junction with the chloroform vapor line.

Liquid chloroform is displaced from a glass reservoir (F) by a nitrogen stream. The nitrogen pressure is closely controlled by means of a sensitive regulator (G) in order to maintain a constant pressure at the outlet of the dip tube, and thus at the chloroform outlet. The trap (H) and alumina absorber (I) serve to protect the nitrogen system from chloroform attack.

The displaced chloroform flows through a shut-off (b) and a fritted-glass filter (J) to a dual-range flowmeter (K). The differential pressure is determined from the liquid levels in the inverted manometer (L). This metered stream then flows to a packed vaporizer tube (M), which is immersed in a salt bath (N). Chloroform vapors pass from the vaporizer, through heated glass lines, to the point of mixing with the preheated chlorine and/or nitrogen stream. The combined vapor stream then flows through an air-jacketed reactor tube (O) and is exposed to the light from the lamp (P) and reflector (Q). The gas temperature in the reactor tube is measured by thermometers (c, d) and controlled by adjusting the power input to the various heaters.

The reacted stream flows through a heated line to a condenser (R), then to a condensate receiver (S). The vapors from the receiver pass on through a large bubbler (T), then to a hood vent. Samples are taken by diverting the vapor-liquid product stream into 1,200-ml. potassium iodide absorbers (U). The liquid levels in the sampling cylinder and the bubbler are adjusted in such a way that the pressure drop through the system will not be changed by sampling.

The reactor system itself is shown in some detail in Figure 2. This system is of the elliptical-reflector type, with the lamp and reactor being mounted along the foci of an elliptical cylinder of anodized aluminum.

The reactor tubes were made from 3.77, 4.72, and 7.37 mm. I.D. tubing. These tubes are long enough (about 2 ft.) to provide an ample upstream calming section. Masks of asbestos sheeting are used to vary the length of the illuminated portion. The reactors are mounted in a 1-¼ in. O.D. by 1-1/16 in. I.D. Vycor jacket.

The light source used for the majority of the runs is a General Electric UA-3 "Uviarc" lamp. This high pressure mercury-arc source emits 63.6 w. of radiant energy, with 10.7 w. being in the near ultraviolet range (3,200 to 3,700 Å). The principle dimensions of this lamp are given in Figure 5.

Some data were obtained using a Gates T5F8 "Black Raymaster" lamp. The filter medium which coats this 8-w. source limits the transmitted energy to the 3,000- to 4,100-Å range. This tubular lamp and filter is ⅞-in. O.D. and 10-¾ in. long.

The procedure of the runs is rather straightforward and will not be discussed here in any detail. The apparatus is started up by setting the feed rates at the desired levels, then adjusting the power input on the various heaters until both thermometers at the reactor indicate 100°C. After sufficient time has elapsed to allow the system to reach the steady state (about 10 min.), one or more timed samples of the product are collected. Meter readings and temperatures are recorded during the sampling period.

Aliquots of the aqueous and organic phases of the product sample are analyzed by first titrating the liberated iodine with 0.1 N sodium thiosulfate (starch indicator). The hydrogen chloride is then titrated with 0.02N caustic (bromothymol blue indicator). The pre-

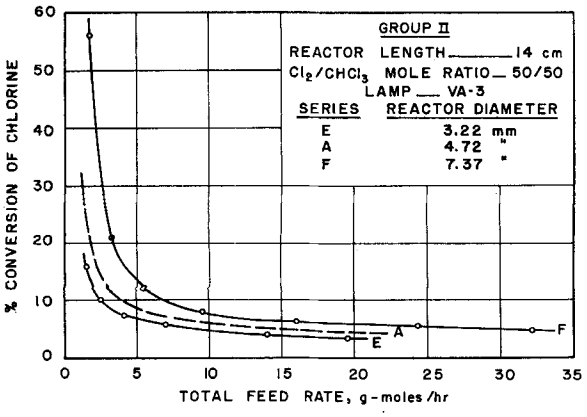

Fig. 4. Variation of reactor diameter, group II.

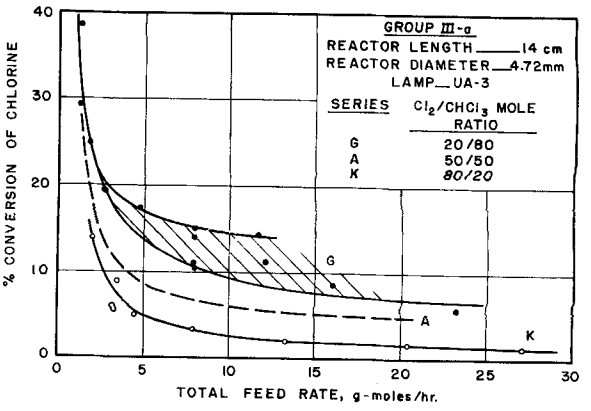

Fig. 5. Variation of reactant ratio, group IIIa.

cision of this method proved to be very satisfactory.

The reagents used in this work were of the highest commercial purity. No elaborate methods of purification were employed, since the use of chemicals and conditions which might be typical of commercial practice was felt to be desirable.

The chlorine used in this work was the standard Matheson cylinder material. As suggested by Pease and Walz (*10*) a portion of the chlorine was vented from new cylinders to remove the bulk of the dissolved impurities.

Chloroform was used throughout this study. A typical analysis of this material is as follows:

Residue after evaporation	4×10^{-4}%
Acetone or aldehyde (as acetone)	10^{-3}%
Lead	10^{-6}%
Ethyl alcohol (preservative)	0.2%

Early lots contained 1% ethyl alcohol, but most of the data were obtained with the above material (all runs after No. 114). Since the alcohol is present in such a low concentration, no further purification was carried out. However it was found that a half-hour nitrogen purge was required (to rid the fresh chloroform of dissolved oxygen) before reproducible results could be obtained.

The nitrogen was the prepurified grade. This material was used without further purification.

The uranyl sulfate and oxalic acid which were used in the actinometric runs were C. P. grade materials. The possible presence of minor amounts of absorbing impurities is of little consequence in this work, since the light transmitted by the actinometric solutions is not an experimental factor.

EXPERIMENTAL RESULTS

The experimental program was carried out by making seventeen series of runs in each of which flow rate was the primary variable. The organization of this program is described in Table 1. A portion of the original data is presented in Table 2. The analytically-determined yields are presented as the mole per cent hydrogen chloride in the inorganic products (hydrogen chloride plus chlorine). This quantity is also equal to the percentage conversion of chlorine and is designated as such in the tables. Partial material balances are presented in Table 2 to indicate the general degree of precision of metering and analysis.

The results of the four principle groups of runs are presented in Figures 3 through 7 as prime-variable plots of the feed rate-conversion data. Two figures (5 and 6) are required for a clear presentation of the data of Group III. With the exception of Series G (Figure 5), the curves are mutually consistent and quite smooth. The comparatively wide scatter in Series G indicates that some unappreciated condition may be quite important in this range of operation.

The degree of precision in the control of the experimental conditions can be illustrated by the results of the two sets of check runs of Series A (Figure 3). These runs were not performed concurrently but were spread out more or less randomly over a forty-four-run program. The degree of precision is quite satisfactory for experiments as complex as those involved here.

The results of the runs at variable reactor lengths (Group I, Figure 3) lead to some interesting observations. For purposes of illustration these data are replotted in Figure 8 as mole fraction hydrochloric acid in the product vs. illumination time. It is interesting to note that all of the data in this group that were obtained at Reynolds numbers greater than 1,800 fall on a single line, within experimental precision. In the laminar flow region however the curves for the various reactor lengths are far from coincident. Since the trends are not well defined in this region, the upper curves merely show the relative positions of the sets of data.

The data show that a discontinuity in rate may occur in the constant-length curves between Reynolds num-

Table 1. Experimental Program

Group	Series	No. of runs	Feed composition, mole % $Cl_2/CHCl_3$	N_2	Reactor I.D., mm.	Reactor L, cm.	Lamp	N_{Re} of feed*
I	A	16	50/50	0	4.72	14	UA-3	660-10,000
	B	6	50/50	0	4.72	7	UA-3	780-10,000
	C	6	50/50	0	4.72	3.5	UA-3	860-10,000
	D	6	50/50	0	4.72	1.75	UA-3	750-10,000
II	E	6	50/50	0	3.22	14	UA-3	1,000-14,000
	A	16	50/50	0	4.72	14	UA-3	660-10,000
	F	7	50/50	0	7.37	14	UA-3	550-10,000
III	G	14	20/80	0	4.72	14	UA-3	780-14,000
	H	10	35/65	0	4.72	14	UA-3	460-15,000
	A	16	50/50	0	4.72	14	UA-3	660-10,000
	J	8	65/35	0	4.72	14	UA-3	830-10,000
	K	9	80/20	0	4.72	14	UA-3	740-10,000
IV	L	5	35/65	0	4.72	26	T5-F8	800-9,400
	M	6	50/50	0	4.72	26	T5-F8	850-10,000
V	N	2	14/56	30	4.72	14	UA-3	1,200 and 5,000
	O	2	20/20	60	4.72	14	UA-3	1,100 and 5,200
	P	2	35/35	30	4.72	14	UA-3	1,200 and 5,100

* Viscosity based on additive molar fluidities of feed components.

TABLE 2. SAMPLE OF ORIGINAL CHLORINATION DATA FOR GROUP *I*, SERIES A

Illuminated reactor length ..... 14 cm.
Reactor diameter ..... 4.72 mm.
Nominal $Cl_2/CHCl_3$ mole ratio 50/50
Lamp UA-3

Run no.	Mole % Cl_2 in feed	Total feed rate, g.-mole/hr.	Press., atm.	Reaction temp., °C. inlet/outlet	% conversion of Cl_2	Reynolds number	Illumination time, sec.	Mole fraction HCl in total product stream	Material balance: (Cl_2 + HCl out) ÷ (Cl_2 in)
161	50.1	1.34	1.03	99/101	28.9	659	0.222	0.145	0.979
53	47.4	1.67	1.02	103/101	23.7	839	0.176	0.1120	1.032
160	50.7	2.01	1.03	99/101	17.6	984	0.148	0.0896	1.002
82	48.7	2.30	1.03	100/98	15.3	1,147	0.129	0.0746	1.002
164	50.1	10.07	1.04	100/101	6.01	4,970	0.0297	0.0302	1.025
154	49.4	10.13	1.04	98/100	6.60	5,020	0.0296	0.0327	1.023
130	49.6	15.30	1.05	100/101	6.07	7,540	0.0198	0.0301	1.033
118	50.1	20.4	1.05	100/100	4.51	10,080	0.0148	0.0226	1.015

bers of about 1,800 and 3,000. On Figure 8 the laminar- and turbulent-flow portions of the curves are connected more or less arbitrarily by the lines at a Reynolds number of about 2,000 (upper limit of laminar region). The existence of such a discontinuity in reaction rate can be rationalized by examining the nature of the reaction:

$$Cl\cdot + \text{wall} \xrightarrow{k_a} \tfrac{1}{2}\, Cl_2$$

Since this is a heterogeneous reaction, its rate may be limited by the rate of transfer of chlorine atoms to the wall. If this were the case in the turbulent-flow region, the over-all rate of reaction should show a dependency on Reynolds number, since mass transfer coefficients are generally observed to increase linearly with the Reynolds number in this flow region. Since the data do not exhibit such a trend in the turbulent-flow region, it can be concluded that:

1. The rate of deactivation of chlorine atoms at the wall is limited by a velocity-independent surface reaction, or
2. Variations in the rate of deactivation of chlorine atoms at the wall have little effect on the over-all reaction rate.

The data are insufficient to allow either possibility to be positively excluded. However the first possibility leads to a more consistent interpretation of the results.

In the laminar flow region the mechanism of mass transfer becomes one of molecular diffusion. Since the rate of mass transfer by diffusion is of a lower order of magnitude than that observed in turbulent mixing, the rate of deactivation of chlorine atoms may well be limited by the rate of diffusion of chlorine atoms to the wall. Thus the rate of wall deactivation would become slower in the laminar-flow region and would therefore be less important in determining the over-all rate of reaction. On this basis a discontinuity in the slope of the curves of Figure 8 would be expected to occur at a Reynolds number of about 2,000. The observed decrease in the rate of reaction as the flow passes from laminar to turbulent would also be expected.

Another interesting observation can be made in regard to the high curvature of a portion of the line representing the turbulent-flow data of Figure 8. This rapid change of reaction rate occurs in the range of contact times from 0.01 to 0.015 sec. It is possible that these high rates result from the chlorination of the ethyl alcohol present in the chloroform feed. However since the difference between results obtained at two alcohol levels (0.2 and 1% in chloroform) are well within experimental error, the effect of this compound cannot be determined. Thus the existence of this initial high-rate period is not explained.

ACTINOMETRIC STUDIES

Interpretation of the chlorination experiments requires that the intensity of illumination reaching the inside walls of the reactors be known. This was determined with the oxalic acid-uranyl sulfate actinometer. These determinations were made by passing a solution 0.05 molar in oxalic acid and 0.01 molar in uranyl sulfate through the reactors at rates which gave conversions of oxalic acid of less than 20%. Under such conditions the decrease in oxalic acid concentration is a measure of the rate of light absorption. Variations in feed rate were found to have little effect on the rate of conversion of oxalic acid. The results of these experiments are given in Tables B1 and B2.*

Consider a tubular reactor of radius R and length L, uniformly illuminated from the outside by a source which emits n_L quanta of light of wave-length λ per unit time. It is assumed that all light rays pass perpendicularly through the axis of the tube and that the concentration of the absorbing species is essentially constant throughout the reactor. The ratio of light absorbed by the reacting stream to the light incident on the inside wall of the reactor will be given by the Beer-Lambert law [Equation (12)]. The moles of oxalic acid decomposed per unit time is

$$M = (C_o - C')\, u\, \pi R^2 = \phi n_a \quad (16)$$

(Note that velocity gradients have no effect on conversion for zero-order reactions, and intensity gradients have no effect for reactions first order in I_a). However since the light source used here is polychromatic and the quantum efficiency is dependent on wave length, it is necessary to apply these equations to narrow wave-length bands and then obtain the total rate of decomposition of oxalic acid by a summation:

$$M = \sum_{\Delta\lambda=1}^{j} (\phi n_a)_{\text{mean}} \quad (17)$$

The spectral distribution of the light from the experimental lamps is given in Table C1,* along with the necessary data on quantum efficiency and absorption coefficients. For the calculation of the incident light intensi-

* Tables labeled with letter and number combinations are on file as document 7082 and may be obtained from the American Documentation Institute, Photoduplication Service, Library of Congress, Washington 25, D. C., for $3.75 for photoprints or for $2.00 for 35-mm. microfilm. The A tables contain the chlorination data, B and C tables the actinometric calculations and data, D tables the chlorine absorption calculations, and E tables some intermediate results in the calculation of rate constants.

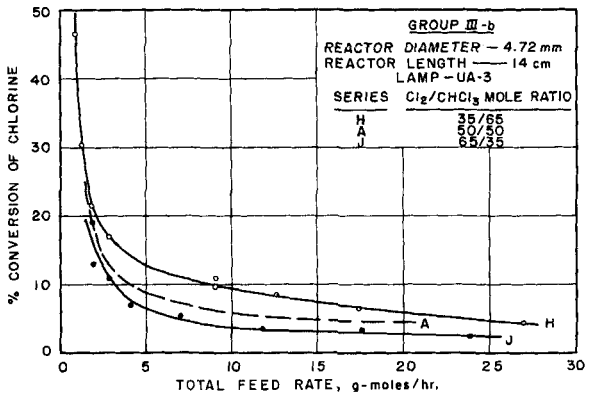

Fig. 6. Variation of reactant ratio, group IIIb.

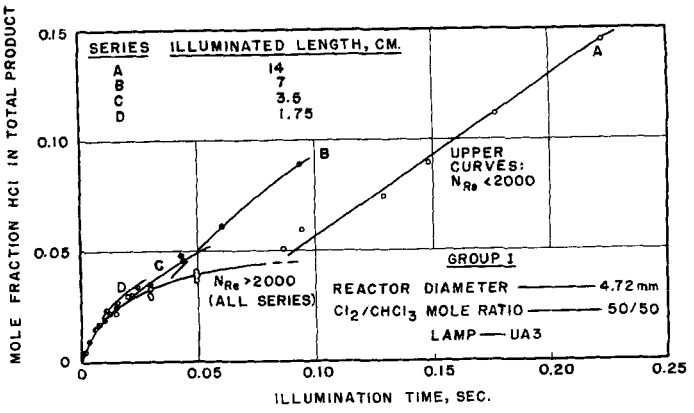

Fig. 8. Product concentration vs. time, group I.

ties from these data Equation (17) is used in the form

$$\frac{M}{\tau} = \sum_{\Delta\lambda=1}^{j} [\phi\,(n_a/n_o)\,(n_o/\tau)] = \sum_{\Delta\lambda=1}^{j} [\phi\,(n_a/n_o) n_L] \quad (18)$$

The fractional transmission efficiency of the optical arrangement is assumed to be nearly independent of wave length, since the reflectance of anodized aluminum and the transmission through Vycor tubing are only slightly dependent on wave length in this region.

To use Equation (18) the fractional absorption is calculated from Equation (12) for a given wave-length band. This ratio is then multiplied by the values of ϕ and n_L for this same band. The products for each band are then summed to give the value of M/τ. Since M is known from Table B2,* τ can be evaluated. When one knows τ, the incident light intensities can be calculated for each wave-length band.

The results of such calculations for the data of Table B2 are summarized in Table C3.* It will be observed that any consistent trend in the results for the UA-3 lamp is removed when these results are expressed in the intensity units. For simplicity the average value of the incident intensity of 0.0014 Einsteins/hr. sq. cm. will be used for each reactor. Thus for the UA-3 lamp

$$N_o = \sum_{\Delta\lambda=1}^{j} n_o = 1.4 \times 10^{-3}\,\pi\,DL \quad \text{Einsteins/hr.} \quad (19)$$

For the T5F8 lamp

$$N_o = 6.4 \times 10^{-6}\,\pi\,DL \quad \text{Einsteins/hr.} \quad (24)$$

Certain of the wave lengths of emission of the lamps are not efficient for the photoactivation of chlorine. Anderson (*1*) has shown that the effective wave lengths lie in the range 3,340 to 4,358Å. for the chlorination of an oil. Since the emission of both lamps used here is quite small near the extremes of this range, the actual limits to be used are not critical. The range of effective wave lengths will therefore be taken as 3,200 to 4,400Å. It will be assumed that variations in the primary quantum efficiency k_1 over this range are small enough that they can be ignored.

For a given value of the quantity CD, Equation (12) can be used with the data of Table C1* to evaluate the fractional absorption of quanta for each wave-length band in the effective range. Since the values of n_L and τ are known for each lamp-reactor combinations (Tables C1 to C3),* the rate of absorption of quanta can then be determined for each increment. The total rate of absorption is the sum of these incremental rates, or

$$N'_a = \sum_{\Delta\lambda=1}^{j}{}' [n_L\,\tau(n_a/n_o)] \quad (21)$$

The primes are used to signify wave lengths in the range 3,200 to 4,400Å.

Equation (21) is used as the basis for estimating the rates of absorption for each of the reported chlorination runs. The actual computations were simplified by using the following equations for mean rates of absorption per unit reaction volume:

UA-3 lamp:

$$I_a = (1.42/D)[1\text{-}10^{-(17.1-262CD)(CD)}] \quad (22)$$

T5F8 lamp:

$$I_a = (0.115/D)[1\text{-}10^{-(34.8-290CD)(CD)}] \quad (23)$$

The results obtained from Equations (22) and (23) are numerically equal, over the range of experimentation, to those obtained from Equation (21).

* See footnote on page 197.

* See footnote in column 1.

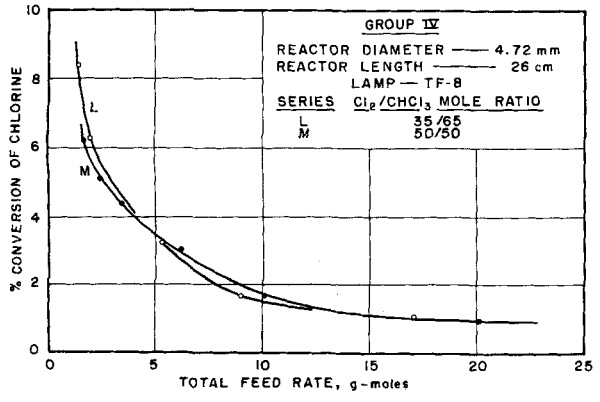

Fig. 7. Variation of reactant ratio, group IV.

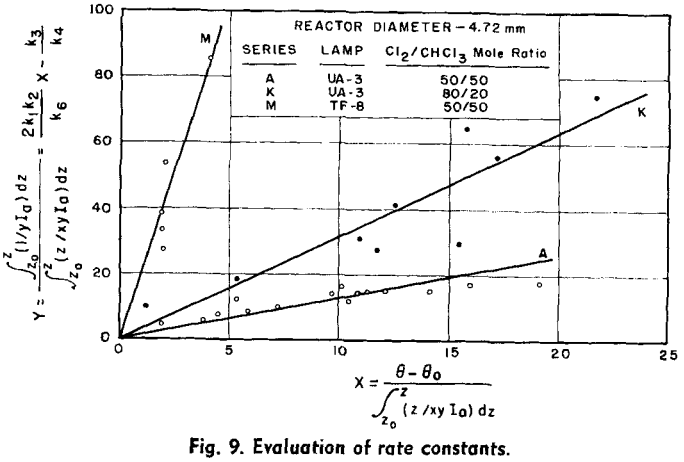

Fig. 9. Evaluation of rate constants.

INTERPRETATION OF CHLORINATION DATA

The quantitative interpretation of the chlorination data depends on the evaluation of the rate constants in the proper kinetic equation. It will be sufficient for the purposes of this discussion to illustrate the extent to which the data deviate from the simplified mechanisms represented by Equations (9) and (10). Such deviations can best be illustrated by determining the trends in the values of the calculated rate constants for each mechanism.

Equation (9) may be written in the form

$$\int_{\theta_o}^{\theta} dt = \int_{(HCl)_o}^{(HCl)} \frac{d(HCl)}{2k_1 I_a + k_4\sqrt{(k_1/k_5)(Cl_2)\, I_a}} \quad (24)$$

This equation can be simplified by neglecting the term $2k_1 I_a$. This is a reasonably good approximation in the present case, since, this term represents a rate of reaction of less than 0.01 mole-fraction/sec. for the conditions of the data of Figure 8. It will be noted that the minimum slope on this figure represents a reaction rate of about 0.4 mole-fraction/sec. When this term is neglected and concentrations are expressed in mole-fractions, Equation (24) becomes

$$k_4\sqrt{k_1/k_5} = \frac{\sqrt{\rho}\int_{z_o}^{z} dz/\sqrt{x\, I_a}}{(\theta - \theta_o)} \quad (25)$$

When the concentrations in Equation (10) are expressed in mole-fractions, there is obtained

$$\left[\frac{\int_{z_o}^{z}(1/y\, I_a)\, dz}{\int_{z_o}^{z}(z/xy\, I_a)\, dz}\right] = \left[\frac{(\theta - \theta_o)}{\int_{z_o}^{z}(z/xy\, I_a)\, d}\right]\left(\frac{2k_1 k_2}{k_5}\right) - \left(\frac{k_3}{k_4}\right) \quad (26)$$

This equation can be checked by calculating values of the bracketed terms from the data by graphical integration. The two groups of constants can then be evaluated from the slope and intercept of an arithmetic plot of the bracketed groups.

The existence of an initial high-rate period in this reaction was discussed in the previous section. Steps must be taken to avoid the influence of this high initial rate on the values of constants calculated from the stationary state kinetics. This initial period can be excluded from consideration by a proper choice of the lower time limit θ_o. The selection of this limit can be rather arbitrary, since the only restriction is that θ_o be greater than the time that is required for the initial high-rate period to pass, provided that the corresponding value of z_o is known.

The lower limits that are used for integration of Equations (25) and (26) were arrived at by first selecting the value for Series A, B, C, and D from Figure 8. Appropriate values for the other series were estimated from the observation that θ_o seems to be inversely proportional to the chlorine concentration in the feed. The resulting values were adjusted as seemed desirable to be near a data point (and to assure the exclusion of the initial-rate period). The corresponding values of z_o are then determined from Figures 3 through 7. Since the data of Series N, O, and P are insufficient to establish the character of the rate curves, the lower limits for integration are set equal to zero.

TABLE 3. APPROXIMATE AVERAGE VALUES OF $k_4\sqrt{k_1/k_5}$ IN EQUATION (25), SEC.$^{-1/2}$

Series	Re <2,000	Re >2,000	Relative magnitude of I_a
A	9.6	8.5	8
B	16	—	8
C	15	—	8
D	(20)*	—	8
E	12	12	8.5
F	9.6	7.5	7.5
G	9.6	(17)	3.5
H	11	13	6
J	8.5	9.6	9
K	8.5	8.5	12
L	15	16	1
M	15	20	1.3
N	(17)	(21)	2.5
O	(7.5)	(13)	3.5
P	(9.6)	(19)	6

* Brackets indicate single values.

TABLE 4. CALCULATED VALUES OF THE CONSTANT $k_4\sqrt{k_1/k_5}$ FOR SERIES A

Run	N_{Re}	Mean contact time, sec.	$k_4\sqrt{k_1/k_5}$ (sec.)$^{-1/2}$
161	660	0.222	12.5
53	840	0.176	10.8
160	980	0.148	9.6
82	1,150	0.129	8.9
156	1,610	0.0941	9.0
57	1,690	0.0862	7.1
147	2,940	0.0496	7.9
141	2,960	0.0491	7.5
159	2,980	0.0491	9.0
144	2,990	0.0493	6.6
137	3,020	0.0488	8.3
121	4,910	0.0301	5.7
164	4,970	0.0297	6.8
154	5,020	0.0296	10.2
130	7,540	0.0198	12.7

The numerical integrations are straightforward and simple but extremely time consuming and tedious by slide-rule methods. Therefore the entire program was carried out with a digital computer.

As shown by Equation (26) the suitability of Equation (10) for use as a model in the interpretation of these data can be tested by plotting the bracketed terms. For Equation (10) to be valid, such a plot must correlate all the data by a single straight line of positive slope and negative intercept, where

$$\text{slope} = 2k_1 k_2/k_5$$

$$\text{intercept} = -k_3/k_4$$

Three series of runs corresponding to widely differing experimental conditions are plotted on Figure 9. The points are fairly well represented by straight lines for each series, probably owing to the use of the integral method of interpretation. However these lines are far from coincident.

The suitability of Equation (9) as a model can be determined from the relative constancy of the group $k_4\sqrt{k_1/k_5}$. Considerable variation of the calculated values within a series of runs would be expected from the nature of the curves of Figure 8. The proper criterion then is the variation between series, rather than the variation within a series. The approximate values of the average of the calculated constant $k_4\sqrt{k_1/k_5}$ are given in Table 3. The results for the viscous-flow region are presented separately, since the curves of Figure 8 show different behavior in this region. The bracketed terms in the above tabulation represent single values, rather than averages. The few values that are obviously extreme are not included in these averages.

The extent of variation of the constants within a series can be seen from the values given in Table 4 for the data of Series A. In general high values are observed at the extremes of contact times for all series of runs. Such high values at low contact times likely reflect the uncertainty in determining the value of the reference concentration z_o at θ_o from the trend lines of Figures 3 through 7. Since the range of contact times varies from series to series, the comparison of Table 3 is not strictly fair to the model. Actually the absence of extreme variations in the constant over the wide range of experimental conditions represented in the above table leads to the conclusion that the model is quite good. Therefore the primary effects of feed composition, feed rate, reactor dimensions, and the spectral distribution and in-

tensity of incident light on the extent of reaction are quite well represented by Equation (9). The fitness of this equation leads to the further conclusion that the rate of free-radical deactivation is largely determined by the rate of the homogeneous termination, step 5. It cannot be concluded however that the deactivation of chlorine atoms at the wall, step 6, is of no importance in this study. In fact this reaction must be considered in order to explain certain secondary effects of the experimental conditions.

The heterogeneous deactivation step would be expected to be most significant under conditions of high turbulence, high chlorine concentration, and high light intensity. In general the trends in the calculated values of the group $k_4\sqrt{k_1/k_5}$ support this contention. Thus the calculated values for the turbulent region show a marked increase (decrease in rate of step 6) when the relatively weak T5F8 lamp is used (Series A vs. M and H vs. L). A slight increase in the extent of wall deactivation in the turbulent region (decrease in over-all rate) is also observed as chlorine concentration increases in Group III (Series G, H, A, J, K). A similar trend is less distinguishable in the laminar-flow region, thus supporting the contention that the significance of this reaction decreases as turbulence disappears.

Two possible shortcomings of the methods of this section for the laminar flow case are:

1. The effects of radial concentration gradients on over-all reaction rates are not considered.

2. The reference point (θ_o, z_o) determined from the turbulent-flow data may not be realistic for the kinetics in laminar flow.

It is possible on the basis of certain assumptions to formulate expressions which take into account these two factors. This was attempted, and the result was partially successful in providing a better correlation of the data in the laminar flow region.

This approach yields values of the rate constant K of 18 for the data of Series A (Table 2), as compared with an average value 9.6 as determined from Equation (25). This higher value is more consistent with the proposed explanation for the observed differences in rate between the laminar- and turbulent-flow regions. The results are not presented here because of space considerations.

CONCLUSIONS

Data on the photochlorination of chloroform in a continuous flow system can be interpreted in terms of the conventional mechanisms applying to light-initiated chain reactions, appropriate definition of the light-absorption rate, and the general principles of flow reactors.

The experiments in this work indicate the effects on reaction rate of feed composition, feed rate, reactor diameter, reactor length, and spectral distribution and intensity of incident light. It is found that the primary effects of these independent variables are explained successfully by a mechanism in which the main termination step is the homogeneous reaction:

$$2C\,Cl_3\cdot + Cl_2 \rightarrow 2C\,Cl_4$$

However to explain certain secondary effects of the data it is necessary to consider also the termination step:

$$Cl\cdot + \text{wall} \rightarrow \tfrac{1}{2}\,Cl_2$$

This reaction appears to be more significant under conditions of higher turbulence and higher light intensity or chlorine concentration.

ACKNOWLEDGMENT

The authors wish to thank E. I. du Pont de Nemours and Company for their support of a portion of this work.

This paper is based on a dissertation submitted by James E. Huff to the Faculty of the School of Engineering of Yale University in partial fulfillment of requirements for the degree of Doctor of Engineering.

NOTATION

C = concentration, moles/liter (C_o = initial concentration)
C' = measured concentration of a component in the product
D = inside diameter of reactors
d = distance in absorbing medium
E = Einsteins, or g.-molecular numbers of quanta
I_a = absorbed light intensity in E/hr. liter
j = index
K = group of rate constants
k = rate constant, or absorption coefficient
L = illuminated length of reactors
M = moles of a substance reacted per unit time
N = photon count over entire lamp spectrum, quanta per unit time
E/hr.-liter of reactor volume
sub. a = absorbed light
sub. o = incident light
sub. t = transmitted light
sub. L = emitted by lamp
N' = photon count in 3,200 to 4,400Å. band
n = photon count over narrow wave-length band
R = inside reactor radius
r = radial distance from reactor axis
t = time variable
u = mean velocity of flow
v = reactor volume
x = mole fraction chlorine
y = mole fraction chloroform
z = mole fraction hydrogen chloride
z_o = experimental value of z at θ_o
( ) = concentration of a compound, moles/unit volume

Greek Letters

Δ = increment
θ = illumination time (contact time), sec.
θ_o = lowertime limit for integrations
λ = wave length of light
ϕ = moles oxalic acid decomposed per quanta absorbed
ρ = vapor density, mole/liter
Σ = summation
Σ' = summation over 3,200 to 4,400Å. wave length region
τ = light transmission efficiency for given optical arrangement (fractional)

LITERATURE CITED

1. Anderson, W. T., Jr., *Ind. Eng. Chem.*, **39**, 844-6 (1947).
2. Baginski, F. C., D. Eng. dissertation, Yale Univ., New Haven, Connecticut (1951).
3. Beezhold, W. F., and L. S. Ornstein, *Physica*, **3**, 154-72 (1936).
4. Doede, C. M., and C. A. Walker, *Chem. Eng.*, **62**, No. 2, pp. 159-178 (Feb., 1955).
5. Gaertner, R. F., and J. A. Kent, *Ind. Eng. Chem.*, **50**, No. 9, pp. 1223-6 (1958).
6. General Electric Co., *Bulletin No. LS-104.*
7. Governale, L. J., and J. T. Clark, *Chem. Eng. Progr.*, **52**, No. 7, pp. 281-285 (1956).
8. Newton, T. W., and G. K. Rollefson, *J. Chem. Phys.*, **17**, 718-25 (1949).
9. Noyes, W. A., Jr., and P. A. Leighton, "The Photochemistry of Gases," Reinhold, New York (1941).
10. Pease, R. N., and G. F. Walz, *J. Am. Chem. Soc.*, **53**, 3728-37 (1931).
11. Schechter, R. S., and E. H. Wissler, Paper presented at the 52 Annual Meeting of the Am. Inst. Chem. Engrs., San Francisco, California (Dec., 1959).
12. Schumaker, H. J., and K. Wolff, *Zeits. f. physik. Chemie*, **(B)25**, 161-76 (1934).
13. Schwab, G. M., and U. Heyde, *ibid.*, **(B)8**, 147-58 (1930).
14. Winning, W. I. H., *Trans. Faraday Soc.*, **47**, 1084-8 (1951).

Manuscript received March 9, 1961; revision received September 19, 1961; paper accepted September 25, 1961. Paper presented at A.I.Ch.E. Lake Placid meeting.